Growth mechanisms of vapor-born polymer films

I. J. Lee,* Mira Yun, Sang-Min Lee, and Ja-Yeon Kim
Department of Physics, Research Institute of Physics and Chemistry, Chonbuk National University, Jeonju 561-756, Republic of Korea
(Received 29 July 2008; published 23 September 2008)

The surface morphologies of poly(chloro-*p*-xylylene) films were measured using atomic force microscopy and analyzed within the framework of the dynamic scaling theory. The evolution of polymer films grown with fixed experimental parameters showed drastic changes in dynamic roughening behavior, which involve unusually high growth exponent ($\beta=0.65\pm0.03$) in the initial growth regime, followed by a regime characterized by $\beta\sim0$, and finally a crossover to $\beta=0.18\pm0.02$ in a steady growth regime. Detailed scaling analysis of the surface fluctuation in Fourier space in terms of power spectral density revealed a gradual crossover in the global roughness exponent, analogous to a phase transition between two equilibrium states, from a morphology defined by $\alpha=1.36\pm0.13$ to the other morphology characterized by $\alpha=0.93\pm0.04$ as the film thickness increases. Our experimental results which significantly deviate from the well established descriptions of film growth clearly exhibit that the dynamic roughening of polymer film is deeply affected by strong molecular interactions and relaxations of polymer chains.

DOI: 10.1103/PhysRevB.78.115427 PACS number(s): 68.47.Mn, 81.15.Aa, 81.15.Kk

I. INTRODUCTION

Organic electronic devices have attracted considerable attention on account of their wide range of present and potential applications, including flexible, transparent, and large-area electronic systems.[1–3] Owing to numerous endeavors to enhance the functionality of the organic devices, several important aspects of the growth dynamics of organic semiconductor[4–6] and the chemical effects at the semiconductor/polymer interface[7–9] are now quite well understood. But relatively little is known about the basic principle governing the temporal evolution of the growth front of polymer film itself.[10–12] In general, the performance of the electronic devices based on organic semiconductors is sensitive to the roughness of dielectric film.[13] Here, we report on the surprisingly rich growth dynamics and morphological characteristics of polymer films grown by vapor deposition. Even with fixed experimental conditions, the dependence of the morphological parameters as a function of the film thickness revealed unprecedented crossovers in the patterns of growth fronts and in their temporal evolutions. The present findings provide a spectacular example of manifestation that the instabilities in the morphological patterns in polymer films were driven by strong molecular interactions and relaxations.

Poly(chloro-*p*-xylylene) (PPX-C) is a transparent plastic film and is the most widely used member of polyxylene derivatives (known by the trade name Parylene) due to its excellent chemical and physical properties. Parylene is used in a broad range of areas, including electronics, medical, aerospace, and industrial applications.[14] In particular, the capacity of PPX-C to form uniform coating as well as its high dielectric strength (>500 V/1 μm) (Ref. 14) make this polymer film a promising candidate for use as a dielectric insulator in applications requiring a thin, transparent, and flexible film.[2,3]

II. EXPERIMENT

PPX-C were deposited in a custom built chemical vapor deposition reactor consisting of a sublimation furnace, a pyrolysis furnace, and a deposition chamber backed by a diffusion pump. Dimer molecules (dichloro-*p*-xylylene) of granular type were sublimed at 120 °C and then cracked into monomers in the pyrolysis furnace at 660 °C. The monomers were subsequently condensed and polymerized on SiO_2/Si substrates in the deposition chamber, which is held at room temperature. The initial interface width (or rms roughness) of the clean SiO_2 surface was typically given as 1.5 Å. Several atomically clean substrates were arranged on a substrate holder which was equipped with a grease-sealed shutter to prevent impurities and volatile contaminants of the dimer molecules from condensing on the substrates during the evacuation of the entire deposition system and during the initial warming up of the sublimation chamber. We found that the use of a substrate shutter providing water leak-tight sealing is crucial to monitor the early stage of island formation in a steady experimental condition. The growth of film stops when closing the shutter and filling the chamber with nitrogen gas to 1 atm pressure. During the deposition, the pressure was typically in the range of 1–3 mTorr, which gave a growth rate of 20–30 nm/min. Each film grown with the same experimental condition was used for various characterizations of the surface, including spectroscopic ellipsometry for determination of the film thickness and x-ray photoemission spectroscopy (XPS) for chemical analysis. The surface morphology was measured using atomic force microscopy (AFM) (PSIA, model XE100) in a noncontact mode. Topographic AFM images were taken from several different locations on each PPX-C film with various scan sizes in the range of 0.5×0.5 to 5×5 μm^2 depending on the film thickness. XPS measurements (AXIS Nova from Kratos) on several films showed that they had chemical compositions very close to the formula composition of PPX-C, without any trace of oxygen contamination. The lack of oxygen contamination, which occurs due to the termination of polymer chain ends by hydroxyl or carbonyl groups during or after the deposition, indicates that our polymer films were of exceptionally high quality.

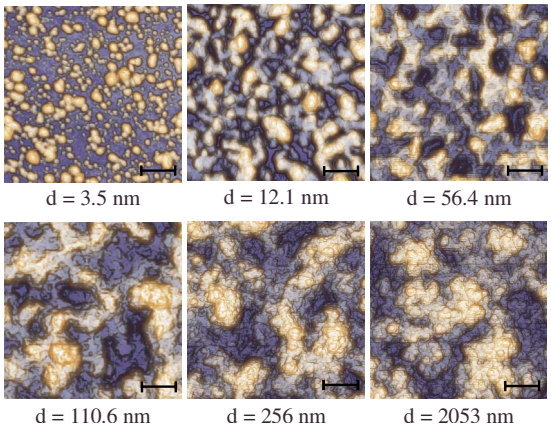

FIG. 1. (Color online) Evolution of topographic AFM images of PPX-C films. The scale bar corresponds to 200 nm in all panels.

III. RESULTS AND DISCUSSION

Representative AFM images taken at various stages of PPX-C film growth are shown in Fig. 1. Islands with rounded edges form during the early stage of growth and then coalesce as the thickness increases. Height histograms obtained from the AFM images indicate three characteristic regimes: (1) the partially covered regime (thickness $d < 14$ nm), in which the bare surface height contributes to the histogram (see the inset of Fig. 2); (2) the regime of asymmetric height distribution associated with deep valleys ($14\ \text{nm} < d < 150$ nm); and (3) the continuous growth regime above 150 nm, where the height distribution is symmetric. For the partially covered regime ($d < 14$ nm), the thickness of the film was determined by averaging the mean-height values from the histograms of several AFM images taken from different locations on each film after the contributions from the bare substrate had been subtracted.

The interface width of the film at different stages of growth is shown in Fig. 2(a). The data were obtained by measuring the root-mean-square fluctuation in height h, $W(L,d)=\sqrt{\langle[h(r)-\langle h\rangle]^2\rangle}$, where L is the scan size and $\langle\cdots\rangle$ denotes a statistical average over the whole scanned area. Although the roughening processes that occur during the growth of film are microscopically diverse and complex in nature, it has been well established that the evolution of interface width follows a simple dynamic scaling called Family-Vicsek scaling relation,[15] expressed as $W(L,d) \sim L^{\alpha} f(d/L^{z})$ where $z=\alpha/\beta$. Determination of the scaling exponents, namely, the roughness exponent α and the growth exponent β, allows one to identify the universality class of the growth process under study.[16,17] Typically, the evolution of interface width has two regimes depending on the length scale L, that is, $W(L,d) \sim d^{\beta}$ for small film thicknesses and $W(L,d) \sim$ const (saturate) for large film thicknesses when the correlation length ξ is comparable to the system size L. Thus, under an experimental condition where $\xi \ll L$, as in our case (see Fig. 4), the interface width as a function of film thickness is expected to follow a simple power-law dependence without saturation. In PPX-C film, however, the interface width as a function of film thickness [Fig. 2(a)] seems far more complicated than what we would expect from the typical growth process. Rather, as noticed in the histograms of the AFM images, three characteristic regimes are observed as the film grows. In the early rapid growth regime, the interface width grows with $\beta=0.65$, much faster than the random deposition limit of stochastic roughening ($\beta=0.5$). Upon complete coverage of the substrate near $d \sim 10$ nm, the film grows with $\beta \sim 0$. In this regime, the interface width does not evolve with the film thickness, which is likely due to preferential filling of deep valleys (the valley filling effect). Note that this is a *rare display of an extreme case of valley filling effect*, which is strikingly different from the phenomenon described by the usual curvature-driven diffusion model or the fourth-order linear molecular-beam epitaxy (MBE) equation.[16,18–20] Finally, the film enters the continuous growth regime, in which the interface width increases steadily with a new power law of $\beta=0.18$.

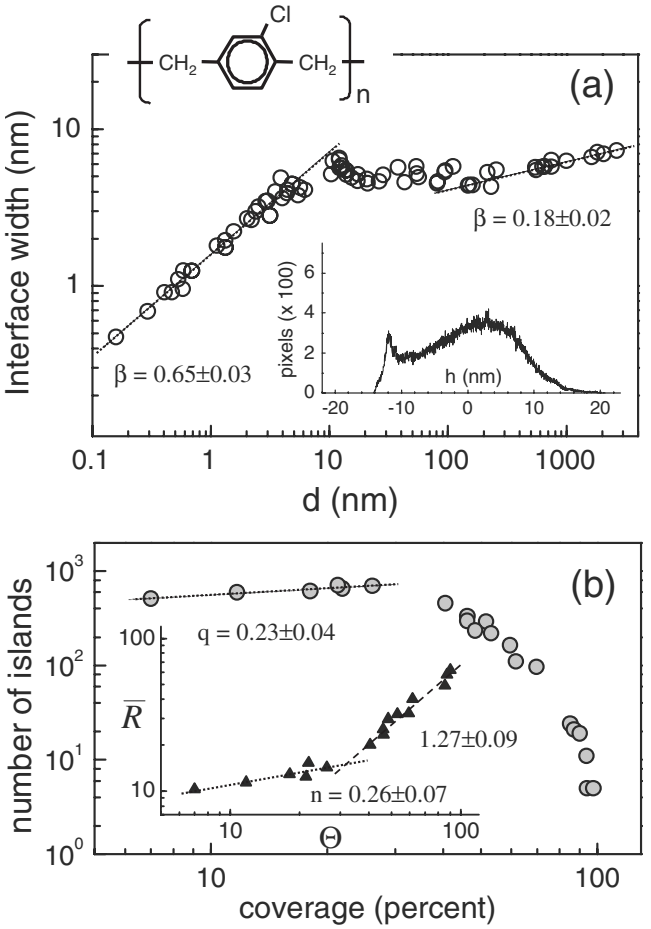

FIG. 2. Top panel: (a) interface width vs thickness of the PPX-C film. The dotted lines are guides for the eyes. Top inset shows the chemical structure of PPX-C. The bottom inset displays the height histogram of $d=11.70$ nm. Bottom panel: (b) number of island as function of coverage Θ. The inset (filled triangles) shows the average island size $\bar{R}$ as function of Θ.

Continuum equations describing film growth involve terms for deposition, desorption, and various diffusions. A crossover in the roughening process can be expected when the competition between different growth mechanisms generates a characteristic length scale in which a particular effect dominates the process.[16,21,22] With a choice of appropri-

ate coupling strength, these models display crossover effects from one dynamics at small time (or short length scale) to another dynamics at long time (or large length scale). However, the evolution of growth dynamics exhibiting this proposed crossover is hard to realize in practice when experimental conditions are fixed, since the crossover length scale (or deposition time) is usually given as either too short or too long to reach within usual experimental ranges.[16] In fact, a few cases of reported crossover effect, such as the laser deposited polymer film[11] and the chemical vapor grown SiO_2 film,[23] were attributed not to the competing growth mechanisms but to nonlocal shadowing effects that drive the growth unstable in early time with unusually high growth exponent ($\beta \geq 0.5$) before the systems undergo continuous stable growth. Particularly, in the studies of polymer films[11] grown by pulsed laser deposition, the crossover was explained in terms of a transition from a single-particle character to a diffusion-driven continuous growth process when the film thickness becomes comparable to the size of the large initial polymer fragments impinging on the flat substrate. The mechanisms underlying the crossovers observed for bisphenol A polycarbonate (BPAPC) film are likely to be different from that observed for the PPX-C film in the present work because the vapor deposition process of PPX-C does not generate large polymer particles in air. Nevertheless, considering that film growth is a bottom-up process, we expect the structure and form of islands on an initially flat surface to exert profound effects on the patterns and dynamics of the subsequent growth front. In the following, we are trying to convince that the intrinsic nature of polymerization process[24,25] characterized by strong interaction between extremely reactive monomer molecules and free-radical polymer chain ends, and relaxation of polymer chain through interpolymer interactions is responsible for the observed unusual growth behavior.

A detailed analysis of the morphology of the PPX-C films during the early stage of growth is shown in Fig. 2(b). Data were obtained from 1 μm^2 AFM images comprised of 512 pixels. Island growth generally involves growth of existing islands, the creation of new islands, and the coalescence of islands. According to a theoretical model for MBE based on the point-island rate equation,[26,27] the number of island (N) and the mean linear island size ($\bar{R}$) are expected to depend on the coverage following the power laws $N(\Theta) \sim \Theta^q$ and $\bar{R} \sim \Theta^n$, respectively. When the islands are small and isolated in the early stage of growth, the number of islands increases as the coverage increases. During the later stage of growth, when the coverage approaches a full layer, the number of islands rapidly decreases due to the merging of clusters. In the intermediate regime where both island nucleation and coalescence occur simultaneously, the balance between the two processes determines the values of the exponents q and n and leads to the relation $q+2n=1$. Figure 2(b) shows that island coalescence is prominent at coverages above 30%, as indicated by the rapid reduction in N and steep increase in $\bar{R}$. However, the measured exponents below the coalescence regime are too low to satisfy the simple relation. The main reason for the failure of the MBE description is that the molecules that land on top of an island contribute to neither N nor $\bar{R}$. Because the diffusion barrier (or Schwoebel barrier[28]) is usually negligible at the step edge of an amorphous polymer film due to the lack of well-defined atomic steps at the surface,[29] the strong molecular interactions, between strongly reactive monomer and free-radical polymer chain ends, and relaxations (or interpolymer interactions) should play a major role in the unusual overgrowth behavior and result in the rapid roughening in our system. Indeed, the rounded edges of the islands (see Fig. 1) and the unusual overgrowth behavior, which lacked in the previous Monte Carlo study[30] considering only monomer surface diffusion, should be a counterexample that proves the presence of strong relaxations which cause entanglement of polymer chains in a way of maximizing the number of nearest neighbors.

Once the surface is nearly covered, the deep valleys between islands, where the density of extremely reactive chain ends is high, are preferentially filled by monomer radicals. After the large variation of local curvature of the interface diminishes, the growth process finds a new equilibrium, which leads to the final transition to the continuous growth regime. The valley filling effect generating an opposite effect of shadowing[31,32] is indeed another manifestation of the presence of strong molecular interactions and long diffusion length in polymer film growth. It is important to note that the nonlocal shadowing effect and step edge barriers, well-known causes for the most of rapid roughening ($\beta > 0.5$) phenomena,[28,29,31,32] are practically excluded in PPX-C system as a possible explanation for the rapid growth of the interface width ($\beta=0.65$). We also like to point out that the coarse graining mechanism observed in an interesting simulation study by Vree and Mayr[33] who considered polymer interactions with the reptation type of relaxation[34,35] nicely captures an essential part of the observed rapid roughening behavior. Even though those interpolymer and intrapolymer interactions produce effects similar to the effects of shadowing and step edge barriers, we expect that the former will cause unusual morphologies and polymer configurations. In following, we deal in detail about the peculiar morphological characters found in polymer films.

The unusual dynamics of the roughening process is also reflected in the evolution of the roughness exponents that characterizes the surface morphology in the stationary regime. Power spectral density (PSD) plots recorded at various thicknesses are shown in Fig. 3. The k dependence in the high-k regime crosses over to a saturation (k-independent) regime at $k_c \sim 1/\xi$ as the surface features lose their correlation. The value of k_c decreases with the film thickness as $k_c \sim 1/d^{1/z}$, where z is the dynamic exponent. The best fit of the k_c vs d plot was achieved using a value of $1/z = 0.21 \pm 0.03$ which was consistent with the value obtained from the real-space relationship between the correlation length and the thickness $\xi \sim d^{1/z}$ (see Fig. 4).[36] The dynamic scaling behavior of the two-dimensional surface is modified in the PSD as $S(k) \sim k^{-(2\alpha_s+2)} d^{2(\alpha-\alpha_s)/z}$ for $k \gg 1/\xi$,[37,38] in which α_s and α are the spectral and the global roughness exponent, respectively. The spectral roughness exponents, which were obtained $[\alpha_s=(m-2)/2]$ by measuring the slope (m) of the k-dependent PSD plot in the high-k regime, are

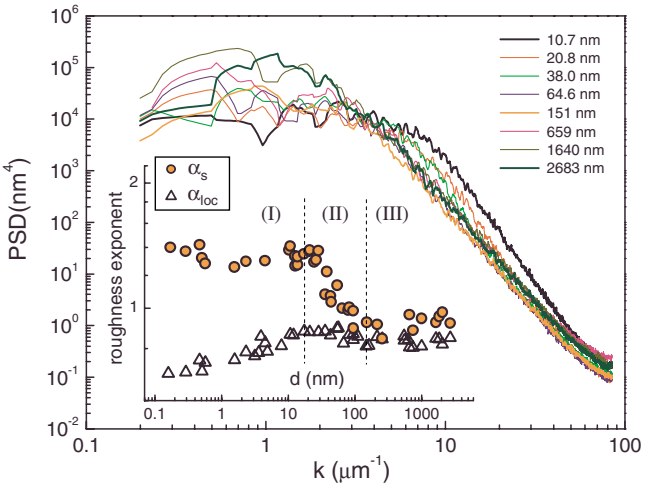

FIG. 3. (Color online) The PSD at various film thicknesses. All of the PSD spectra are based on the AFM images of 3 μm^2 scans. The inset shows the thickness dependence of the spectral (α_s) and the local (α_{loc}) roughness exponents.

shown as filled circles in the inset of Fig. 3. The local roughness exponents marked by open triangles were obtained by fitting the height-difference correlation function $H(\mathbf{r}) = \langle [h(\mathbf{r}) - h(\mathbf{0})]^2 \rangle^{1/2}$ to $\rho r^{\alpha_{loc}}$ for small r regime ($r \ll \xi$).[16] The self-affinity of the interface, a conventional assumption of the normal scaling behavior, is lost when the global scaling differs from the scaling behavior of the local interface width, that is, $\alpha \neq \alpha_{loc}$.

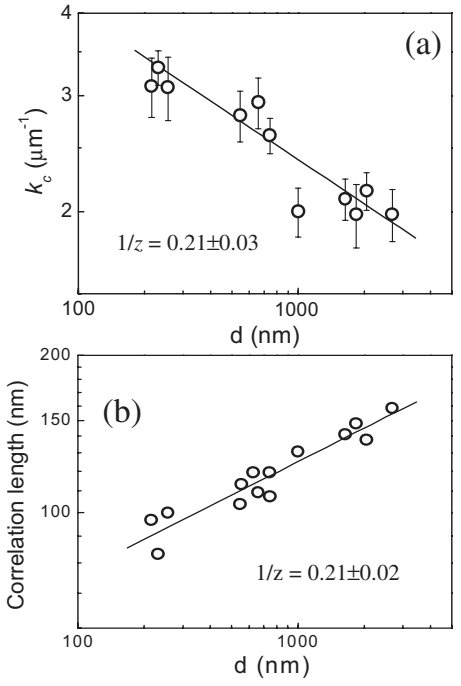

FIG. 4. (a) The thickness dependence of the crossover k_c obtained from PSD functions of the AFM images of 3×3 μm^2 size. The linear fit (solid line) yields the dynamic exponent $1/z = 0.21 \pm 0.03$. (b) The correlation length as a function of film thickness. The slope of the linear best fit is displayed as a solid line and yields $1/z = 0.21 \pm 0.02$.

In regime (I), the PSD in high-k region varies negligibly with the film thickness ($\alpha = \alpha_s$) and α is substantially different from α_{loc}, which lead to the relation $\alpha_s = \alpha \neq \alpha_{loc}$. The scaling behavior of regime (I) is thus anomalous and belongs to the super-roughing process since $\alpha = 1.36 \pm 0.13 > 1$. In the valley filling regime (II), the dynamic scaling behavior is quite complex that the PSD curves shift downward ($\alpha < \alpha_s$) and the slope of the k-dependent PSD continuously decreases with increasing film thickness as shown in Fig. 3. The scaling relationship $\alpha_s \neq \alpha \neq \alpha_{loc}$ is satisfied in this intermediate regime and, interestingly, does not belong to any of the classes that have been identified for interfacial growth.[16,37,38] This unprecedented scaling behavior has not been found in usual atomic deposition process and is likely associated with the intrinsic properties of polymer formation. But the precise role of strong interpolymer and intrapolymer interactions in the unusual scaling behavior is yet to be unfold. It is also very hard to understand the fact that, in this new class of growth regime, the local exponent remains the same while the global exponent continuously decreases with the film thickness. In the continuous growth regime (III), the PSD curves are thickness invariant, indicating that $\alpha = \alpha_s$ and the scaling exponents are obtained as $\alpha_s = 0.93 \pm 0.04$ and $\alpha_{loc} = 0.85 \pm 0.03$. The small difference between α_s and α_{loc} appears to be real since multiaffine behavior is clearly visible in this regime.[39] In other words, the interface cannot be characterized by a single roughness exponent.[16] The dynamic scaling behavior of regime (III) is similar to that of regime (I) in which the relation $\alpha_s = \alpha \neq \alpha_{loc}$ characterizing the super-rough surface holds. It is interesting to note that, even though there is a large difference in the global roughness exponent, both regimes (I) and (III) share the same dynamic scaling properties, which suggest that the strong molecular interaction resulting in the rapid increase as well as the saturation of the interface width persists throughout the entire growth process.

As we may expect from the complex scaling properties and various crossovers which are significantly different from those of conventional film growth such as MBE, assigning a universality class for the polymer film growth is not trivial. The measured exponents $\alpha = 0.93 \pm 0.04$, $\beta = 0.18 \pm 0.02$, and $1/z = 0.21 \pm 0.02$ in the continuous growth regime compare only marginally, at best, with those obtained from both the linear ($\alpha = 1$, $\beta = 0.25$, $1/z = 0.25$) (Refs. 18 and 19) and the nonlinear MBE equation ($\alpha = 0.67$, $\beta = 0.2$, $1/z = 0.3$) (Refs. 40–43) in 2+1 dimensions. The clear differences between the observed and the compared are a strong indication that polymer film growth is very different from the conventional MBE growth process. If we neglect all the detailed differences, the local curvature-induced diffusion term ($K\nabla^4 h$) contained in both the MBE models is responsible for the conventional scaling in reciprocal space ($\alpha = \alpha_s$) and the anomalous behavior in real space ($\alpha \neq \alpha_{loc}$) (Refs. 19 and 37) as we have observed. The involvement of curvature-driven diffusion term in polymer growth seems plausible because local valleys of the interface where density of active chain ends or number of nearest neighbors is high make a favorable place for both monomer radicals and usual atoms to stick. However, we note that a series of higher order nonlinear terms must be included in the picture to account for

the unusual multiscaling behavior.[40,44] The reasoning is partly consistent with the argument of Punyindu and Das Sarma[45] against the conclusion drawn from previous studies of the similar polymer films (PPX) in which nonlocal bulk diffusion was suggested[12] as a governing mechanism in the continuous growth regime.

IV. SUMMARY

We have studied the kinetic roughening of vapor-deposited PPX-C films over a film thickness range encompassing more than 3 orders of magnitude. The rapid growth in the early stage and crossover to the saturation of interface width which significantly deviate from the conventional MBE description were understood in line with strong molecular interaction and relaxation of polymer chains. The characteristic exponents in the continuous growth regime were cross-checked with independent methods and consistently obtained as $\alpha=0.93\pm0.04$, $\beta=0.18\pm0.02$, and $1/z=0.21\pm0.02$. As we have discussed, the scaling exponents cannot be directly related to any known universality classes based on conventional atomic deposition. In light of previous theoretical studies of polymer growth[30,33] which specifically designed for a linear-chain polymer, our experimental results suggest that a successful polymer model should incorporate the intrinsic properties of polymer growth such as strong interaction between monomer radicals and polymer chain ends and relaxation of polymer chains. Certainly, polymer systems should provide a myriad of possibilities for learning more about the formation of rough fronts and their evolution beyond the MBE process. Finally, since the peculiar growth behaviors of PPX-C films come from the intrinsic properties of polymerization process, we expect to see unusual growth behavior in other linear-chain polymers. However, we note that different chemical compositions of polymer should provide ranges of interaction strength which essentially determines the behavior of kinetic roughening (see, for example, Ref. 12, in which unusual growth behavior was argued for bulk diffusion). So far, our studies have raised more questions than answers regarding the growth mechanism of polymer film. We hope the present experimental study will stimulate the interest in polymer growth.

ACKNOWLEDGMENTS

We thank S. M. Jeong and M. Ha for valuable discussions. This work was supported by the Korea Science and Engineering Foundation under Grant No. R01-2006-000-10800-0 and by the Korea Research Foundation under Grant No. KRF-2005-015-C00135.

*ijlee@chonbuk.ac.kr

[1] N. Stutzmann, R. H. Friend, and H. Sirringhaus, Science **299**, 1881 (2003).
[2] K. Nomura, H. Ohta, T. Kamiya, M. Hirano, and H. Hosono, Nature (London) **432**, 488 (2004).
[3] T. Someya, Y. Kato, T. Sekitani, S. Iba, Y. Noguchi, Y. Murase, H. Kawaguchi, and T. Sakurai, Proc. Natl. Acad. Sci. U.S.A. **102**, 12321 (2005).
[4] F.–J. Meyer zu Heringdorf, M. C. Reuter, and R. M. Tromp, Nature (London) **412**, 517 (2001).
[5] L. F. Drummy and D. C. Martin, Adv. Mater. (Weinheim, Ger.) **17**, 903 (2005).
[6] A. C. Mayer, A. Kazimirov, and G. G. Malliaras, Phys. Rev. Lett. **97**, 105503 (2006).
[7] K. P. Pernstich, S. Hass, D. Oberhoff, C. Goldman, D. J. Gundlach, B. Batlogg, A. N. Rashid, and G. Schitter, J. Appl. Phys. **96**, 6431 (2004).
[8] M.-H. Yoon, C. Kim, A. Facchetti, and T. J. Marks, J. Am. Chem. Soc. **128**, 12851 (2006).
[9] C. Kim, A. Facchetti, and T. J. Marks, Science **318**, 76 (2007).
[10] G. W. Collins, S. A. Letts, E. M. Fearon, R. L. McEachern, and T. P. Bernat, Phys. Rev. Lett. **73**, 708 (1994).
[11] J. Hachenberg, C. Streng, E. Suske, S. Vauth, S. G. Mayr, H. U. Krebs, and K. Samwer, Phys. Rev. Lett. **92**, 246102 (2004).
[12] Y.-P. Zhao, J. B. Fortin, G. Bonvallet, G.-C. Wang, and T.-M. Lu, Phys. Rev. Lett. **85**, 3229 (2000).
[13] S. Steudel, S. De Vusser, S. De Jonge, D. Janssen, S. Verlaak, J. Genoe, and P. Heremans, Appl. Phys. Lett. **85**, 4400 (2004).
[14] W. F. Beach, *Encyclopedia of Polymer Science and Technology*, 3rd ed. (Wiley, New Jersey, 2004).
[15] F. Family and T. Vicsek, *Dynamics of Fractal Surfaces* (World Scientific, Singapore, 1990).
[16] A.-L. Barabasi and N. E. Stanley, *Fractal Concepts in Surface Growth* (Cambridge University Press, Cambridge, England, 1995).
[17] J. Krug, Adv. Phys. **46**, 139 (1997).
[18] J. G. Amar, P.-M. Lam, and F. Family, Phys. Rev. E **47**, 3242 (1993).
[19] S. Das Sarma, S. V. Ghaisas, and J. M. Kim, Phys. Rev. E **49**, 122 (1994).
[20] The curvature diffusion models with conserved noise which give the saturated interface width in $2+1$ dimensions are not relevant in our case because monomers are permanently attached to polymer chain-ends through chemical bonding.
[21] C. M. Horowitz, R. A. Monetti, and E. V. Albano, Phys. Rev. E **63**, 066132 (2001).
[22] T. J. da Silva and J. G. Moreira, Phys. Rev. E **63**, 041601 (2001).
[23] F. Ojeda, R. Cuerno, R. Salvarezza, and L. Vázquez, Phys. Rev. Lett. **84**, 3125 (2000).
[24] W. F. Beach, Macromolecules **11**, 72 (1978).
[25] J. B. Fortin and T.-M. Lu, Chem. Mater. **14**, 1945 (2002).
[26] J.-K. Zuo and J. F. Wendelken, Phys. Rev. Lett. **66**, 2227 (1991).
[27] J. G. Amar, F. Family, and P.-M. Lam, Phys. Rev. B **50**, 8781 (1994).
[28] R. L. Schwoebel and E. J. Shipsey, J. Appl. Phys. **37**, 3682 (1966).
[29] H. N. Yang, Y. P. Zhao, G. C. Wang, and T. M. Lu, Phys. Rev. Lett. **76**, 3774 (1996).
[30] Y.-P. Zhao, A. R. Hopper, G.-C. Wang, and T.-M. Lu, Phys. Rev. E **60**, 4310 (1999).

[31] R. P. U. Karunasiri, R. Bruinsma, and J. Rudnick, Phys. Rev. Lett. **62**, 788 (1989).
[32] J. Yu and J. G. Amar, Phys. Rev. E **66**, 021603 (2002).
[33] C. Vree and S. G. Mayr, J. Appl. Phys. **100**, 013511 (2006).
[34] P. G. DeGennes, J. Chem. Phys. **55**, 572 (1971).
[35] M. Rubinstein, Phys. Rev. Lett. **59**, 1946 (1987).
[36] The correlation length can be accurately determined from the relation $C(\xi)/C(0)=e^{-1}$ after evaluation of the two-dimensional correlation function $C(\mathbf{r})=\langle h(\mathbf{r})h(0)\rangle$ for each of the AFM images.
[37] J. M. López, M. A. Rodríguez, and R. Cuerno, Phys. Rev. E **56**, 3993 (1997).
[38] J. J. Ramasco, J. M. López, and M. A. Rodriguez, Phys. Rev. Lett. **84**, 2199 (2000).
[39] While the global regime shows simple scaling with an exponent $\alpha=0.93\pm0.04$, the qth order height-difference correlation function $H_q(\mathbf{r})=\langle[h(\mathbf{r})-h(0)]^q\rangle^{1/q}$ exhibits spatial mutiscaling below a length scale of ~ 30 nm at $d=2053$ nm. Details of the properties of the multifractality found in this system will be discussed elsewhere. The exponent α_{loc} shown in the text corresponds to $\alpha_q(q=2)$.
[40] S. Das Sarma and P. Punyindu, Phys. Rev. E **55**, 5361 (1997).
[41] Z.-W. Lai and S. Das Sarma, Phys. Rev. Lett. **66**, 2348 (1991).
[42] D. E. Wolf and J. Villain, Europhys. Lett. **13**, 389 (1990).
[43] S. Das Sarma and P. Tamborenea, Phys. Rev. Lett. **66**, 325 (1991).
[44] J. Krug, Phys. Rev. Lett. **72**, 2907 (1994).
[45] P. Punyindu and S. Das Sarma, Phys. Rev. Lett. **86**, 2696 (2001).